

# Modeling the transport of very short-lived substances into the tropical upper troposphere and lower stratosphere

J. Aschmann<sup>1</sup>, B.-M. Sinnhuber<sup>1</sup>, E. L. Atlas<sup>2</sup>, and S. M. Schauffler<sup>3</sup>

<sup>1</sup>Institute of Environmental Physics, University of Bremen, Bremen, Germany

<sup>2</sup>Rosenstiel School of Marine and Atmospheric Science, University of Miami, USA

<sup>3</sup>National Center for Atmospheric Research, Boulder, Colorado, USA

Received: 14 August 2009 – Published in Atmos. Chem. Phys. Discuss.: 9 September 2009

Revised: 16 November 2009 – Accepted: 17 November 2009 – Published: 7 December 2009

**Abstract.** The transport of very short-lived substances into the tropical upper troposphere and lower stratosphere is investigated by a three-dimensional chemical transport model using archived convective updraft mass fluxes (or detrainment rates) from the European Centre for Medium-Range Weather Forecast's ERA-Interim reanalysis. Large-scale vertical velocities are calculated from diabatic heating rates. With this approach we explicitly model the large scale subsidence in the tropical troposphere with convection taking place in fast and isolated updraft events. The model calculations agree generally well with observations of bromoform and methyl iodide from aircraft campaigns and with ozone and water vapor from sonde and satellite observations. Using a simplified treatment of dehydration and bromine product gas washout we give a range of 1.6 to 3 ppt for the contribution of bromoform to stratospheric bromine, assuming a uniform mixing ratio in the boundary layer of 1 ppt. We show that the most effective region for VLSL transport into the stratosphere is the West Pacific, accounting for about 55% of the bromine from bromoform transported into the stratosphere under the supposition of a uniformly distributed source.

WMO, 2007). In particular brominated VLSL are found to contribute significantly to stratospheric ozone depletion (e.g., Sinnhuber et al., 2009). However, measurements of VLSL are scarce and the estimations of abundance and source strength still remain uncertain.

In this paper we focus mainly on brominated VLSL, particularly bromoform ( $\text{CHBr}_3$ ). According to the estimations published in the WMO (2007) report it is the most abundant VSL bromocarbon. The major part of this compound is emitted naturally from the ocean by maritime lifeforms such as macroalgae, ice algae and phytoplankton groups (Quack and Wallace, 2003). Average bromoform mixing ratios in the marine boundary layer (MBL) are estimated to be in the range of 1 to 2 parts per trillion by volume (ppt) (WMO, 2007) but Quack and Wallace (2003) noted that local mixing ratios can be much higher, especially in tropical coastal regions or in areas which show strong upwelling. The most important sinks of bromoform are photolysis, which dominates at the upper troposphere/lower stratosphere (UTLS), and reaction with the hydroxyl radical at lower altitudes. The average lifetime of bromoform is about 26 days (WMO, 2007).

Various studies were performed to investigate how VLSL are able to reach the stratosphere even though their lifetimes are relatively short in comparison to typical atmospheric transport times (e.g., Nielsen and Douglass, 2001; Warwick et al., 2006; Sinnhuber and Folkins, 2006; Kerkweg et al., 2008; Gettelman et al., 2009). It is generally assumed that the most important pathway of air entering the stratosphere is in the tropics through the tropical tropopause layer (TTL) via convection (e.g., Sinnhuber and Folkins, 2006). Here, the level of zero clear sky radiative heating (at an altitude of about 15.5 km) marks the transition from large-scale subsidence to large-scale ascent, as diagnosed from diabatic

## 1 Introduction

Recent studies have shown the importance of halogenated very short-lived substances (VLSL) to stratospheric halogen loading and their contribution to ozone depletion (e.g.,



Correspondence to: J. Aschmann  
(jaschman@iup.physik.uni-bremen.de)

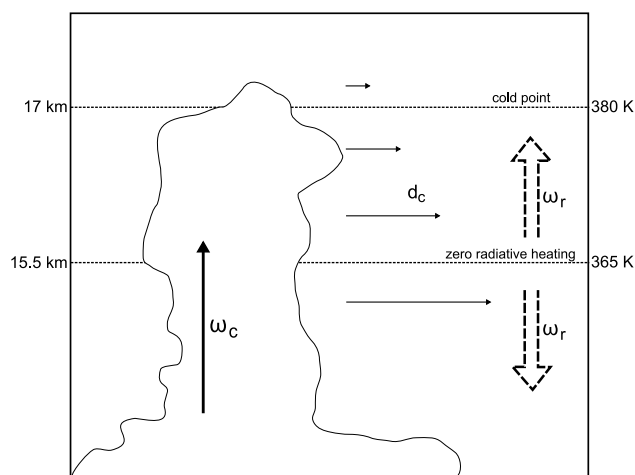


**Fig. 1.** Schematic of relevant transport processes in the TTL. Beside the large-scale vertical transport which is driven by diabatic heating rates  $\omega_r$  there is a fast and localized convective mass flux  $\omega_c$ . The amount of air leaving the convective cloud is given by the convective detrainment rate  $d_c$ . Note that only air parcels detraining above the level of zero radiative heating, the transition between large-scale subsidence to large-scale ascent, are able to reach the stratosphere. At 17 km the TTL temperature profile reaches a minimum (see also Fig. 7). Air parcels traversing this altitude are likely to be subject to dehydration.

heating rates (e.g., Corti et al., 2005) and thus representing a natural border for air parcels (see Fig. 1). In general, air masses have to be lifted by deep convection above this border to leave the troposphere, which is considered to be the common pathway into the stratosphere. Since air lifted by convective clouds is able to rise several kilometers within a few hours this transport mechanism is fast enough for VLSL whose life times are rather in the order of weeks.

Another important process to be considered here is the dehydration of the TTL. At an altitude of about 17 km the average temperature profile reaches a minimum (cold point). Air masses entering the stratosphere must be dehydrated to mixing ratios that correspond roughly to the saturation mixing ratio at this level. This process of dehydration is not fully understood and is still subject to current discussions. Studies indicate (e.g., Holton and Gettelman, 2001; Fueglistaler et al., 2005) that during the relatively slow ascent through the TTL it is highly probable that air masses are transported horizontally into the coldest areas of the tropical tropopause typically residing over the Maritime Continent and Western Pacific regions. The so called cold trap hypothesis states that a major parts of the whole TTL air gets dehydrated in these particular areas. Along with the dehydration of air this implies that a specific amount of soluble species residing in the TTL could eventually be washed out by falling ice. This process is important for modeling bromine compounds since model calculations indicate that a large fraction of total in-

organic bromine ( $\text{Br}_y$ ) is actually HBr and HOBr, which are both highly soluble.

There have already been several modeling studies of VLSL. For example, Nielsen and Douglass (2001) supposed a uniformly distributed bromoform emission over the oceans of approximately 500 Gg/yr which corresponds to a surface concentration between 1 and 2 ppt in their three-dimensional (3-D) model. They concluded that roughly one third of  $\text{Br}_y$  in the UTLS is due to the destruction of  $\text{CHBr}_3$ . Warwick et al. (2006) conducted 3-D model runs with various emission scenarios for bromoform and compared them with observational data. According to their results a scenario which concentrates bromoform emissions of the 500 Gg/yr suggested by Nielsen and Douglass (2001) in the tropical oceans is able to reproduce the observed data thus strengthening the importance of the tropical oceans as source regions for bromine VLSL. Sinnhuber and Folkins (2006) used a 1-D model to give estimations about the amount of bromine reaching the stratosphere taking into account a convective detrainment rate that was calculated by balancing the diabatic heating rate and washout of  $\text{Br}_y$  due to TTL dehydration. They constrained the contribution of bromoform to stratospheric  $\text{Br}_y$  to 0.5 to 3 ppt for an assumed ground level mixing ratio of 1 ppt. More recently, Kerkweg et al. (2008), Gettelman et al. (2009) and Hossaini et al. (2009) further investigated the transport of VLSL with detailed chemistry and convective parametrizations (see Sect. 4).

In our model experiments we use a 3-D chemical transport model (CTM) to simulate the transport of bromine VLSL into the stratosphere. The novelty of our approach is to use an isentropic model with a parameterization of deep convective transport. In contrast to the fast and localized convective mass flux we calculate the slow large-scale vertical motion from diabatic heating rates. With this tool we have studied the effect of dehydration on VSL tracers and investigated the relative importance of different source regions using several emission scenarios.

## 2 Model description

### 2.1 Three-dimensional chemical transport model

The model used here is an updated version of our CTM described by Sinnhuber et al. (2003). It is forced by temperatures and horizontal windfields from ERA-Interim reanalysis of the European Centre for Medium-Range Weather Forecast (ECMWF). The spatial resolution of our runs were  $2.5^\circ$  lat.  $\times$   $3.75^\circ$  lon. with a vertical resolution of 29 isentropic levels between 330 and 2700 K (about 10 to 55 km). We used a timestep of 15 min for all model runs.

Transport on isentropes is calculated from the meteorological wind fields while the large scale vertical motion is derived from diabatic heating rates. In contrast to the before-mentioned earlier CTM version which used

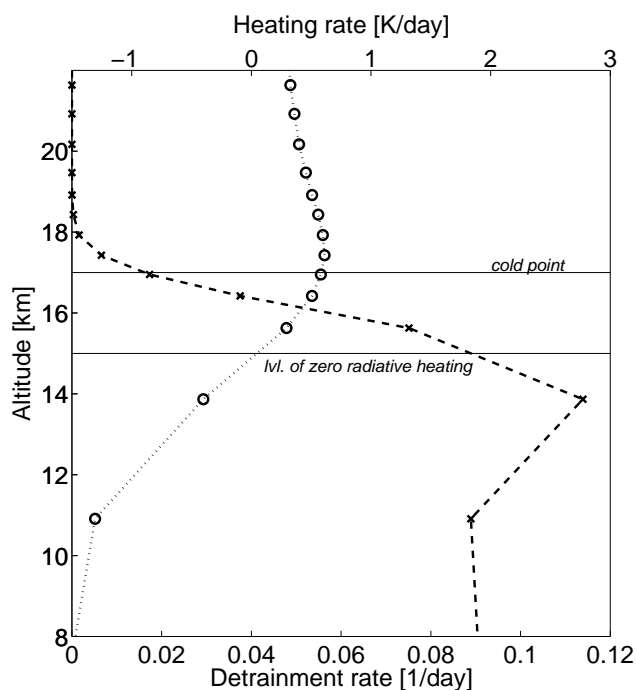


**Fig. 2.** Zonally averaged profiles of ECMWF ERA-Interim detrainment rate (dashed) and diabatic heating rate (dotted) between 20° N and 20° S. These profiles are temporally averaged from 2000 to 2005.

interactive heating rate calculation from an ozone tracer, the current version relies on the ECMWF data for tendency of clear sky long and short wave radiation. They are found to be more accurate in the tropopause region and are (at least in principle) consistent with the large-scale wind fields and convective mass fluxes. However, the ERA-Interim radiative heating rates lack a feedback to interactive ozone (Fueglistaler et al., 2009). Figure 2 shows a zonally averaged profile of the heating rate in tropical latitudes (20° S to 20° N). Fueglistaler et al. (2009) found in the diabatic heat budget of ERA-Interim a residual diabatic cooling in the lowermost stratosphere over the Maritime Continent, most likely due to the model's turbulent mixing parameterization. It remains to be shown if this is a real feature or an artefact and whether or not this is related to cooling by overshooting deep convection. This diabatic tendency is not considered in our CTM calculations. In addition to the relatively slow vertical heating rate-driven advection we have also included a fast convective transport mechanism in our model that will be further discussed in Sect. 2.2.

The tracers which are modeled are ozone, water vapor and two idealized tracers with different chemical lifetimes (5 and 20 days) to resemble typical VSL halogen substances such as methyl iodide ( $\text{CH}_3\text{I}$ ) and bromoform ( $\text{CHBr}_3$ ) which will be further referred to as test tracer 5 and 20 (TT5 and TT20), respectively. Furthermore, there are two tracers for inorganic

bromine ( $\text{Br}_y$ ) which is assumed to be the degradation product of bromoform (ref. to Sect. 2.4). The ozone tracer is calculated by a linearized ozone chemistry which is an updated version of LINOZ (McLinden et al., 2000); treatment of water vapor is described in detail in Sect. 2.3.

We have conducted three modeling experiments with an integration time of 6 years (2000 to 2005) each. The first experiment concentrated on comparison between model calculations and observational data for specific tracers in order to test our approach (Sect. 3.1). As next step we used our model to study the effect of dehydration on the transport of short-lived tracers and their soluble byproducts into the stratosphere (Sect. 3.2). Since convection plays a keyrole in these processes, we also conducted a sensitivity run with the same setup but with convection switched off above 380 K (for further details on our convective transport please refer to Sect. 2.2). Finally, we applied the mechanisms introduced in the second experiment to several emission scenarios to investigate the relative importance of specific source regions (Sect. 3.3).

## 2.2 Convection

As a novel feature of our model we have included a parameterization of convective transport. As noted above, isentropic coordinates have significant conceptual and practical advantages for modeling the large-scale transport in the UTLS. However, because it is difficult to extend a purely isentropic model into the lower troposphere and down to Earth's surface, so far isentropic models either did not include any parameterization of convection at all, or have used a hybrid coordinate where isentropic surfaces are blended with terrain following surfaces in the lower atmosphere (e.g., Rasch et al., 1997; Chipperfield, 2006). Instead of using an interactive convective parameterization, we have parameterized convective transport by using archived convective updraft mass fluxes from the ERA-Interim reanalysis. This approach has the additional advantage that the convective mass fluxes are calculated during the assimilation process in a consistent way. In contrast, when using a convective parameterization inside a CTM, there is always the potential problem that the driving large-scale temperature and pressure fields from the meteorological analysis have already been stabilized by a convective parameterization within the assimilation.

Here we have used the 6-hourly updraft convective mass fluxes from ERA-Interim, or more specifically the updraft detrainment rates, which are the vertical divergence of the updraft convective mass fluxes. An example is shown in Fig. 2. The detrainment rate  $d_c$  gives the convective flux of mass into a grid box per time (unit 1/s). It is derived from the original ECMWF updraft detrainment rate by integration over the model grid box divided by the air density inside the box. Convective injection of tracers is then modeled by specifying a detrainment tracer mixing ratio  $[X]_c$  that multiplied

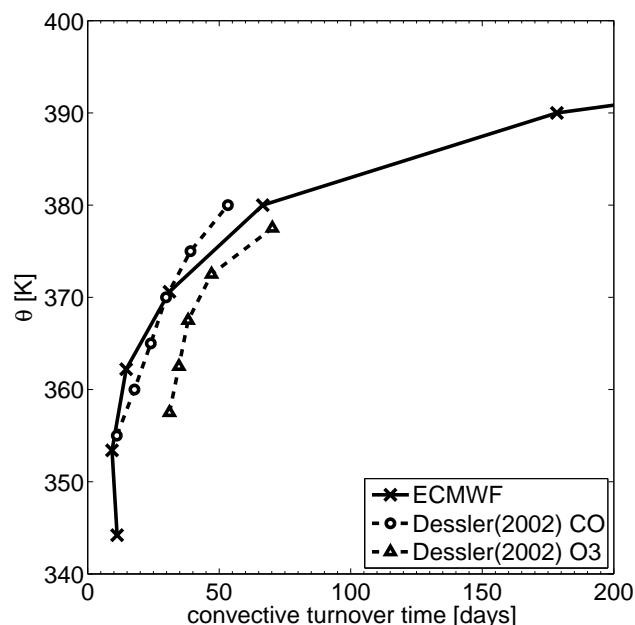


**Fig. 3.** Comparison of tropical averaged convective turnover times derived from the ECMWF detrainment rate (solid) and those calculated by Dessler (2002) from CO (dashed, circles) and O<sub>3</sub> (dashed, triangles) measurements.

with the detrainment rate  $d_c$  and the total grid box mass  $m$  gives the convective tracer flux  $f_{X,c}$  into the grid box:

$$f_{X,c} = d_c \cdot m \cdot [X]_c \quad (1)$$

We assume that the detrainment mixing ratio  $[X]_c$  is similar to the tracer mixing ratio in the planetary boundary layer, but in general entrainment of mid tropospheric air during convective updrafts may also influence the detrainment mixing ratio.

With this model approach we are able to simulate the slow large-scale transport constrained by diabatic heating rates with fast updrafts taking place quasi instantaneously as a sub-grid scale process. However, this approach is not strictly mass conserving, which is the case also in other isentropic CTMs even without convective transport. To force mass conservation the total mass inside a grid box after advection and convection steps is set to the calculated mass from the large-scale meteorological analysis. Tracer masses are scaled proportionally to keep the calculated tracer mixing ratios constant.

Note that  $d_c$  is still significant in the tropics above the level of zero radiative heating and even above the coldpoint at 380 K as it can be seen in Fig. 2. With our approach of convective transport this means a considerable amount of air is detrained at relatively high altitudes and it is unclear, whether this frequent high reaching transport is a realistic representation. However, comparisons of the convective turnover time

derived from ECMWF  $d_c$  with calculations made by Dessler (2002) based on CO and O<sub>3</sub> observations show excellent agreement up to 380 K (Fig. 3). To assess the influence of detrainment above the coldpoint on our model calculations we have conducted a sensitivity run where we cut off the convective transport above 380 K (Sect. 3.2).

### 2.3 Treatment of water vapor

Water vapor plays an important role in our calculations because we need an adequate representation of atmospheric humidity to model possible loss of soluble Br<sub>y</sub> due to washout (Sect. 2.4). Furthermore its distribution in the atmosphere is another convenient means to validate the model assumptions since there are plenty of measurements of this quantity that can be considered. The treatment of the H<sub>2</sub>O tracer is based on three simplistic assumptions: (1) For the convective transport, the source term  $[H_2O]_c$  in Eq. (1) is set to the saturation mixing ratio of water vapor over ice of the particular model box, following Dessler and Sherwood (2004). This corresponds to the assumption, that air detraining from a convective cloud is fully saturated. The saturation mixing ratio is calculated after the formula of Marti and Mauersberger (1993). (2) Likewise, if the relative humidity of a box exceeds 100%, all surplus water is removed immediately thus modeling precipitation as instantaneous fallout of ice particles. (3) Finally there is a second water source in the stratosphere implemented by a simple methane oxidation scheme as described in the ECMWF Integrated Forecast System documentation (IFS Documentation, 2007). The basic supposition is, that the sum of methane and water is constant in the stratosphere and can be approximated by:

$$2[CH_4] + [H_2O] = 6.8 \text{ ppm} \quad (2)$$

Therefore the production of water via methane oxidation can be expressed as:

$$\frac{d[H_2O]}{dt} = \frac{(6.8 \text{ ppm} - [H_2O])}{\tau} \quad (3)$$

Here  $\tau$  denotes a pressure dependent chemical lifetime of methane which is set to 100 days at 50 pa pressure and increases roughly linearly to  $\approx 6000$  days at 10000 pa. Above this mark the lifetime is set to infinity, i.e. the H<sub>2</sub>O production due to methane oxidation is zero at lower altitudes.

### 2.4 Br<sub>y</sub> production and loss processes

As for VSL bromine substances we focus mainly on bromoform (CHBr<sub>3</sub>) and its role in taking bromine to the stratosphere, since it is one of the most abundant VSL bromine species. Stratospheric bromine loading due to bromoform can be divided into processes called source or product gas injection (WMO, 2007). Either the bromine atoms enter the stratosphere directly as bromoform or as its inorganic degradation products, summarized here as Br<sub>y</sub>. The distinction

between source and product gases is important, because unlike  $\text{CHBr}_3$  itself a major part of its degradation products is highly soluble, in particular  $\text{HBr}$  and  $\text{HOBr}$ . Therefore precipitation may remove a significant amount of bromine from the atmosphere.

To investigate these processes we use a simplified approach, however one that is more physically motivated than the use of a fixed washout lifetime used in most of the previous modeling studies. Bromoform is approximated by an idealized tracer (TT20) which has a constant chemical lifetime of 20 days and a constant detrainment mixing ratio of  $[\text{TT20}]_c = 1$  ppt. At each timestep, the amount of TT20 is reduced according to the assumed lifetime which represents the loss of  $\text{CHBr}_3$  caused by photolysis and oxidation. For each unit of TT20 destroyed there are three units of  $\text{Br}_y$  produced in the same grid box thus ignoring the detailed chemistry of bromoform's degradation products, which is according to the recent study of Hossaini et al. (2009) a valid approximation. There is no other source of  $\text{Br}_y$  in our model. The only sink of  $\text{Br}_y$  is supposed to be through washout by falling rain or ice. To avoid the complexity of cloud and aerosol microphysics we investigate the two extremal cases using two different  $\text{Br}_y$  tracers: one is not affected by washout at all, the other is removed completely if dehydration occurs in the particular model grid box. This will give an estimation of the upper and lower limit of stratospheric bromine loading due to bromoform.

### 3 Results

#### 3.1 Comparison with observational data

In order to test whether our new approach in modeling convective and large-scale vertical transport produces realistic results we compared the model output with different observational data. In this particular experiment we used the following tracers: Ozone, water vapor and two idealized VSL tracers.

##### 3.1.1 Very short-lived source gases

The model tracers TT5 and TT20 are idealized VSL tracers that resemble  $\text{CH}_3\text{I}$  and  $\text{CHBr}_3$  regarding to their chemical lifetime, which were assumed to be 5 and 20 days, respectively. Due to their short lifetime the distribution of these tracers in the UTLS is mainly localized at distinct areas where significant convective activity occurs. However, even for very short-lived tracers horizontal transport can be very important in the TTL. Figure 4 shows an example of the distribution of the idealized methyl iodide VSL tracer (TT5).

Profiles of TT5 and TT20 are presented in Fig. 5 together with observational data of  $\text{CH}_3\text{I}$  and  $\text{CHBr}_3$  from NASA WB57 high-altitude aircraft measurements during two Aura Validation Experiment (AVE) campaigns. Both campaigns, Pre-AVE and Cr-AVE, were performed around 80–90° W at

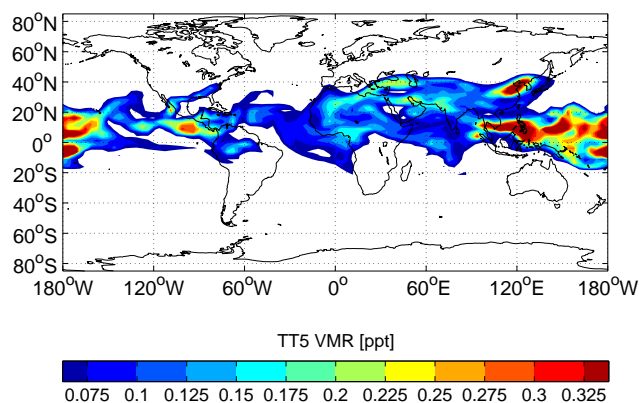


**Fig. 4.** Snapshot of TT5 (idealized  $\text{CH}_3\text{I}$  tracer) distribution at 380 K (about 17 km altitude in the tropics) on 1 August 2003

latitudes between 20° N and 3° S in January/February 2004 and 2006, respectively. The profiles show the mean, the range between minimum and maximum values and the standard deviation over all measurements at the particular altitude. Likewise, the model data from January/February 2004 was averaged over the same area allowing a direct comparison to the Pre-AVE campaign. There is in general good agreement between model calculations of the 5 and 20 day tracers and the Pre-AVE observations of  $\text{CH}_3\text{I}$  and  $\text{CHBr}_3$  if we assume a uniform detrainment mixing ratio of 0.3 ppt and 0.75 ppt, respectively. There is in general also good agreement with the 2006 Cr-AVE observations, although there are also notable differences. These may either reflect real interannual changes or could (in particular for the  $\text{CH}_3\text{I}$  measurements during Cr-AVE) indicate a small high bias in the observations due to a possible residual artifact observed in new canisters that were used during Cr-AVE.

##### 3.1.2 Ozone

Ozone, albeit itself not our primary subject in this paper, is quite suitable to test whether our modeling approach works properly, because there are a lot of observational data available for comparison. In Fig. 6 we compare modeled ozone data with sonde measurements from the Southern Hemisphere Additional Ozonesondes (SHADOZ) project (Thompson et al., 2003). For comparison, we picked measurements from two stations, Watukosek, Java (7.5° S, 112.6° E) and San Cristóbal Island, Galapagos (0.9° S, 89.6° W) and the corresponding model grid boxes. We kept the detrainment mixing ratios  $[\text{O}_3]_c$  constant for all locations at 20 ppb. Even with this relatively simple treatment of ozone, the model reproduces generally well the observed profiles. The difference in convective activity and therefore the different ozone profiles of the two stations are well reproduced by the model. However, especially the modeled profile over the Java region show too low ozone mixing ratios in

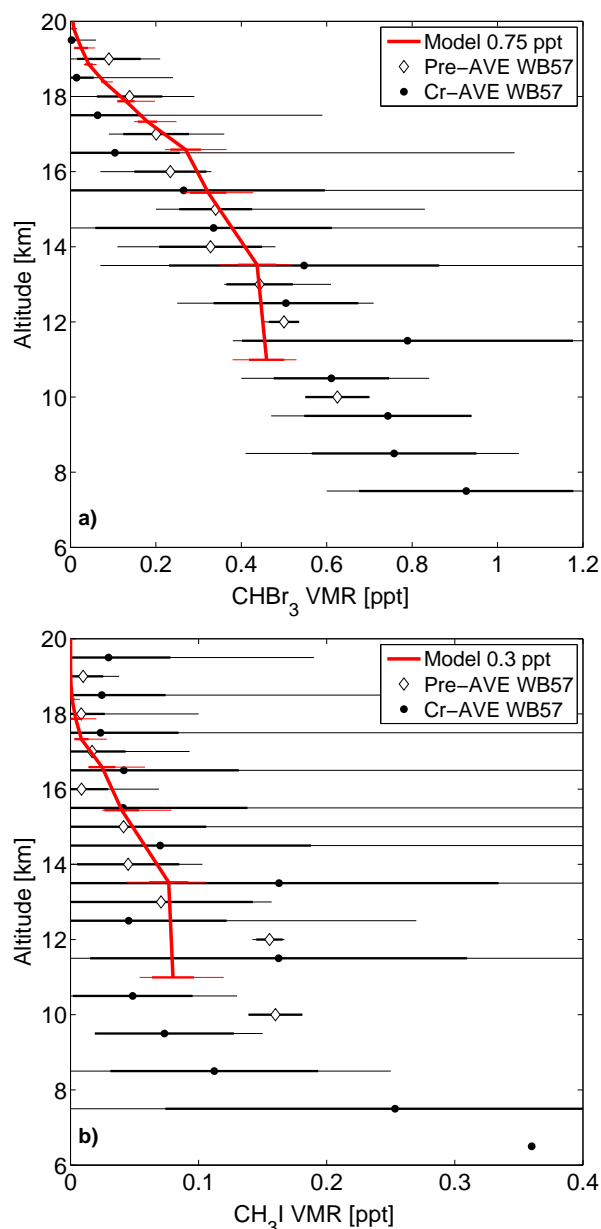


**Fig. 5.** Comparison between modeled  $\text{CHBr}_3$  (a) and  $\text{CH}_3\text{I}$  (b) tracers (TT20 and TT5, resp.) and aircraft measurements from Pre-AVE and Cr-AVE campaign. The observations were performed at about  $80\text{--}90^\circ\text{ W}$ ,  $20^\circ\text{ N--}3^\circ\text{ S}$  during January/February 2004 and 2006, respectively. Both measurements and model data were averaged over this area. Please note that for this comparison we used only model data from January/February 2004 therefore the modeled profile fits especially well to the Pre-AVE campaign observations. The red curves mark modeled profiles while for the observations symbols denote the mean of the individual measurements within a 1 km altitude range. Thick and thin horizontal lines represent one standard deviation and the range between minimum and maximum values of the measurements and the model data, respectively. The detrainment mixing ratio of TT20 was assumed to be 0.75 ppt and 0.3 ppt for TT5.

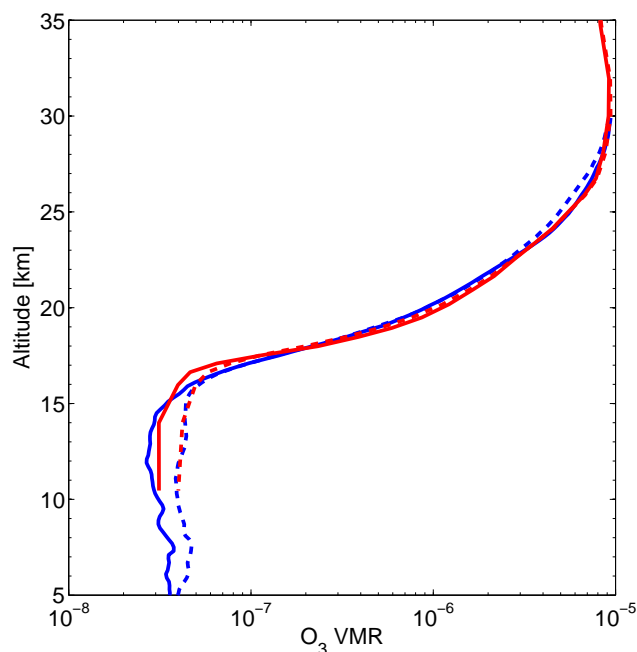


**Fig. 6.** Comparison between modeled ozone profiles (red) and SHADOZ measurements (blue). Shown are yearly averages from 2004. The solid and dashed lines mark profiles from Watukosek, Java ( $7.5^\circ\text{ S}$ ,  $112.6^\circ\text{ E}$ ) and San Cristóbal Island, Galapagos ( $0.9^\circ\text{ S}$ ,  $89.6^\circ\text{ W}$ ), respectively.

the TTL. This could indicate an overestimation of convective transport in our model but may also be a consequence of too little chemical ozone production.

### 3.1.3 Water vapor

Our modeled water vapor agrees generally well with measurements despite the simplistic treatment in our model. In the troposphere the averaged profile of relative humidity with respect to ice (RH) is in qualitative agreement with observations (e.g., Folkins et al., 2002), in particular the decrease of RH with decreasing altitude in the lower TTL (Fig. 7). This decrease in RH results from the large-scale subsidence and associated adiabatic warming of air that was initially saturated at convective detrainment. The successful representation of this effect is thus only possible with the separation of slow large-scale descent and fast isolated convective updrafts in the model. In the stratosphere the modeled water vapor shows a clear tape recorder signal in the stratosphere (Fig. 8). Comparison with HALOE measurements (Groß et al., 2005) show in general excellent agreement in the dry phases and also the speed of the tape recorder signal is well reproduced (Fig. 9). But these comparisons reveal also that in our model too much water (on average by about 1 ppm) is transported into the tropics at altitudes above 17 km during Northern Hemisphere (NH) summer. In our calculations the

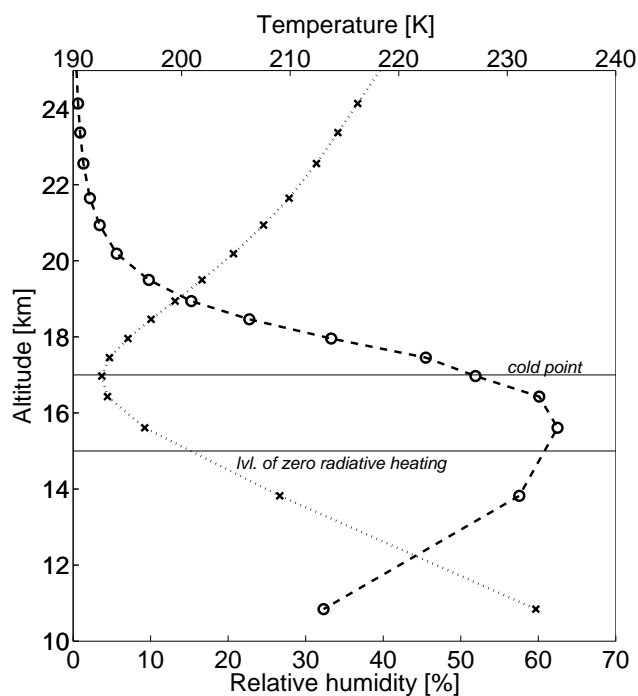


**Fig. 7.** Zonally averaged profiles of modelled relative humidity of water vapor with respect to ice (dashed) and temperature (dotted) between 20° N and 20° S. These profiles are temporally averaged from 2002 to 2005.

“moist head” of the tape recorder is located at about 18 km which is not supported by the HALOE observations. However, other measurements do show high water vapor mixing ratios at 17 km and above in NH summer above mid-latitudes (Dessler and Sherwood, 2004; Hanisco et al., 2007). It is not clear if the discrepancy in water vapor between our model and HALOE observations are a result of too much convective transport above the cold point or whether our assumption that air detrains with 100% RH overestimates the flux of water into the stratosphere. Moreover, a more realistic treatment of dehydration (e.g., Gettelman et al., 2002a; Read et al., 2008) may lead to an improved water vapor representation.

### 3.2 The effect of dehydration on soluble gases

In the second experiment we introduced a pseudo chemistry scheme for our idealized bromoform tracer as stated in Sect. 2.4. Since the product gas tracer Br<sub>y</sub> was modeled to be soluble, dehydration plays an important role in the question which amount of bromine compounds reaches the stratosphere.

Figure 7 shows profiles of modeled relative humidity (RH) and temperature averaged zonally over 20° N and 20° S. Mean RH peaks with 60% at around 16 km which is slightly lower at the important level of minimum temperature, the cold point, at around 17 km. However, local areas show much

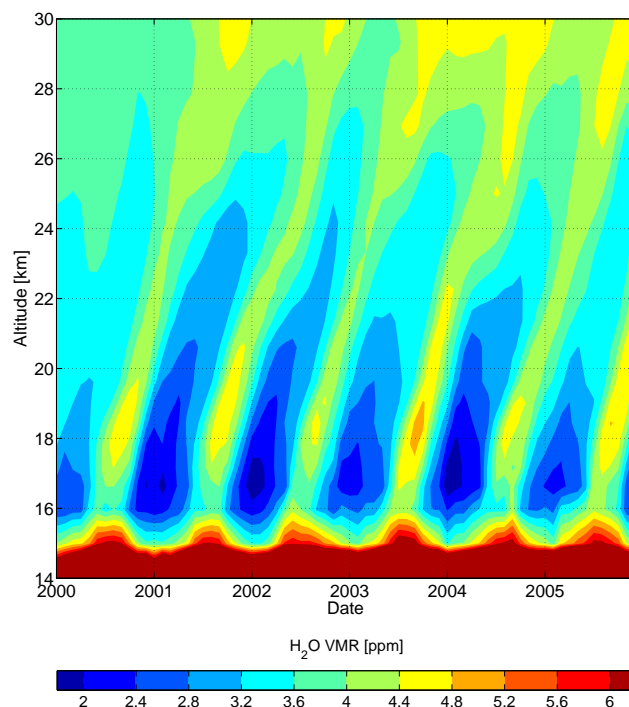


**Fig. 8.** Modeled distribution of tropical water vapor mixing ratio (“tape recorder”) temporally averaged from 2000 to 2005.

higher values for RH, especially during NH summer over the Indian Monsoon and West-Pacific regions. Our model suggests that a significant part of TTL dehydration occurs at these areas which is on the line with the results of Gettelman et al. (2002a) and Fueglistaler et al. (2005).

Under these circumstances, our model suggests an additional bromine loading due to an idealized VSL tracer in the range of 1.6 to 3 ppt as shown in Fig. 10. Here we assume a constant detrainment mixing ratio of the source gas TT20 (CHBr<sub>3</sub>) of 1 ppt. Due to the fact that our soluble Br<sub>y</sub> tracer is subject to dehydration and is therefore directly linked with the water vapor tracer we see also a tape recorder signal in its stratospheric mixing ratio (Fig. 11). Considering the differences of the tape recorder phases and comparing the TT20 and soluble Br<sub>y</sub> profiles we estimate that about 1.2 to 1.3 ppt of the soluble Br<sub>y</sub> is formed above the cold-point (about 17 km or 380 K) and is thus not significantly affected by dehydration. The remaining 0.3 to 0.4 ppt were most likely produced at lower altitudes and are consequently subject to periodical dehydration as seen in the tape recorder plot. Note that these results are not dependent on significant convection above the coldpoint, since our sensitivity run with no convective transport above 380 K produces virtually identical results (Fig. 10). For the estimations we have made above this means that a significant amount of source gas reaches the stratosphere via the slow large-scale upward motion, even if we don’t consider deep convection above 380 K.

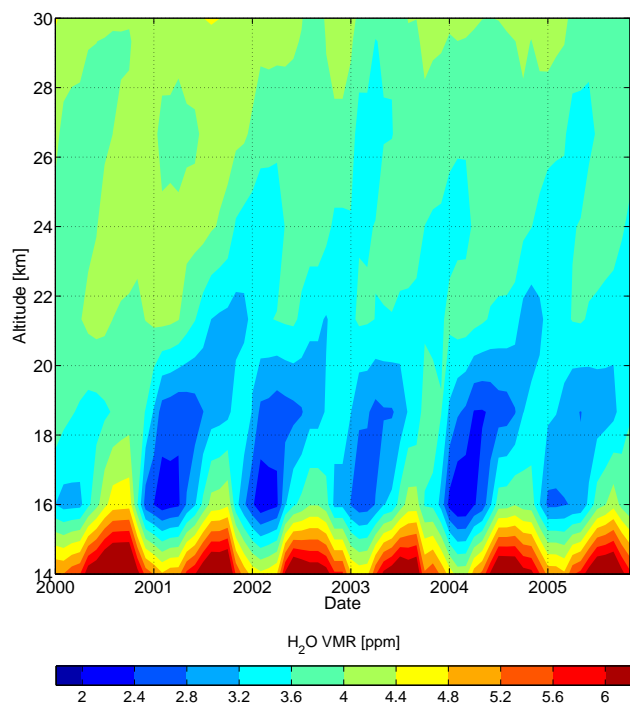


**Fig. 9.** Distribution of tropical water vapor mixing ratio (“tape recorder”) temporally averaged from 2000 to 2005 measured by HALOE (Groß et al., 2005).

### 3.3 Transport efficiency for different source regions

In a third experiment we applied the approach of  $\text{CHBr}_3$  degradation into  $\text{Br}_y$  product gas (ref. Sect. 2.4) to different emission scenarios to investigate their relative importance for stratospheric bromine loading. As shown in Fig. 12 we introduced nine source areas which roughly correspond to Earth’s oceans and continents. Each region is associated with a group of three tracers: one source gas tracer (TT20) and the upper and lower limit product gas tracers (insoluble and soluble  $\text{Br}_y$ , resp.). The detrainment mixing ratio parameter  $[\text{TT20}]_c$  for a particular region is 1 ppt inside and zero outside the corresponding area. Note that this approach only takes the different transport efficiencies into account. In general there will of course be variations in the source strengths between the different regions as well, which is not considered here.

Our model results show clearly that even tracers with a lifetime of only a few days can travel vast horizontal distances in the TTL. Figure 13 illustrates this fact in showing an arbitrary snapshot of the Western Pacific source gas tracer distribution: of course the highest concentrations are located above the emission region but there are also significant mixing ratios thousands of kilometers away above Central America and the Atlantic. Considering this fact it is interesting to return again to the Pre-AVE measurements above Central

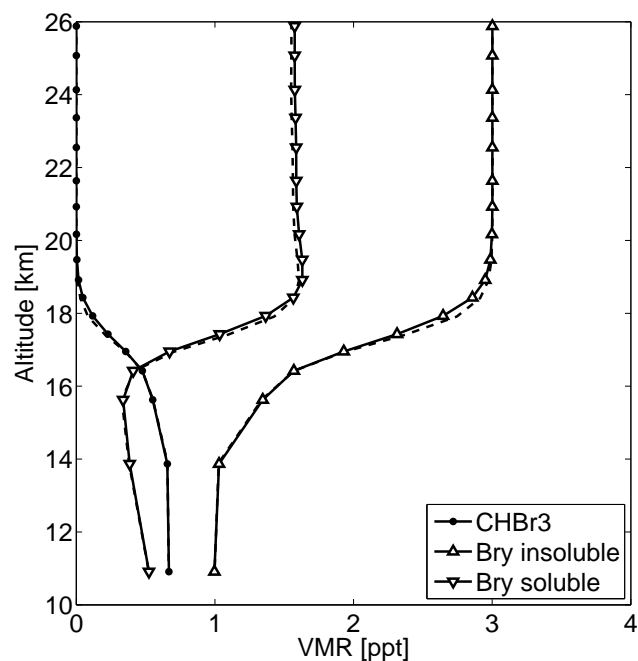


**Fig. 10.** Averaged tropical profiles of idealized bromoform (dots) and insoluble/soluble  $\text{Br}_y$  tracers (upward/downward facing triangle, resp.). The two  $\text{Br}_y$  tracers constrain the stratospheric bromine loading to 1.6 to 3 ppt given the assumption that the source gas  $\text{CHBr}_3$  has a ground-level mixing ratio of 1 ppt. The dashed profiles are derived from a sensitivity calculation where the convective detrainment above 380 K (about 17 km) was switched off.

America conducted in early 2004 (ref. to Sect. 3.1.1). We already showed in Fig. 5, that our model is able to reproduce the observed profile of bromoform in this particular region. We now use our individual source regions approach to investigate their relative contribution to this profile. Figure 14 shows the contribution of the different source regions to the total amount of TT20 in the before mentioned Pre-AVE area drawn against altitude. It indicates that the Western Pacific (WPa) is clearly dominating all other regions, interestingly also the American (Ame) and Eastern Pacific (EPa) sources, in whose areas the observation took place. At lower altitudes, the WPa, EPa and Ame tracers contribute roughly one third of total  $\text{CHBr}_3$  each. At the UTLS, however, the influence of the latter diminish and the WPa tracer makes up about 70%.

As generalization, Fig. 15 shows the relative contribution of the investigated source regions to TT20 for the whole tropics (note that the plot looks virtually the same if made for  $\text{Br}_y$  instead). The picture is similar to the local example presented above: At lower altitudes the relative contribution is roughly equal for most of the source regions whereas at the UTLS the Western Pacific is clearly identified as the most important area which contributes about 55% to the total TT20 abundance. Apparently, the Western Pacific and the Maritime Continent are the only regions where substantial

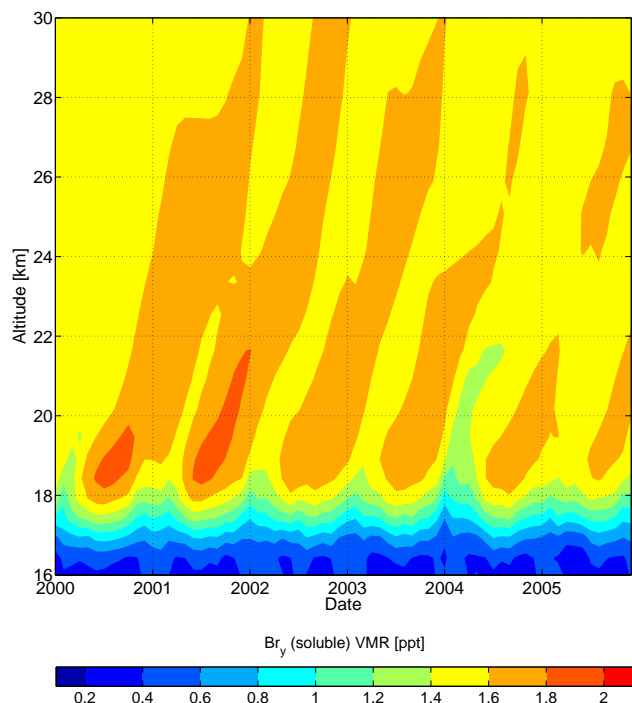


**Fig. 11.** Modeled distribution of tropical  $\text{Br}_y$  mixing ratio temporally averaged from 2000 to 2005. Since  $\text{Br}_y$  is assumed here to be soluble the distribution shows also a ‘tape recorder’ shape.

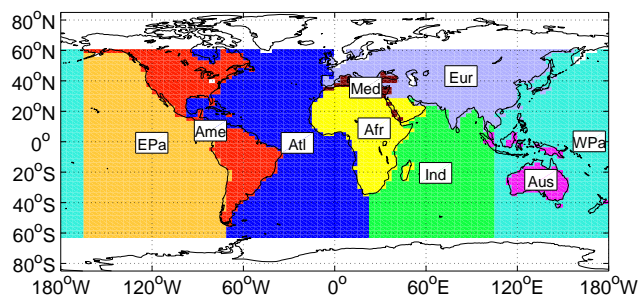


**Fig. 12.** Map of the nine different source regions used in our model. The regions are from left to right: Eastern Pacific (EPa), America (Ame), Atlantic (Atl), Mediterranean (Med), Africa plus Arabian Peninsula (Afr), Indian Ocean (Ind), Eurasia (Eur), Australia plus Maritime Continent (Aus), Western Pacific (WPa).

high-reaching (i.e. above the level of zero radiative heating) convection occurs. Thus these regions represent the most important transport pathway into the stratosphere, in agreement with earlier studies (e.g., Gettelman et al., 2002b; Liu and Zipser, 2005).

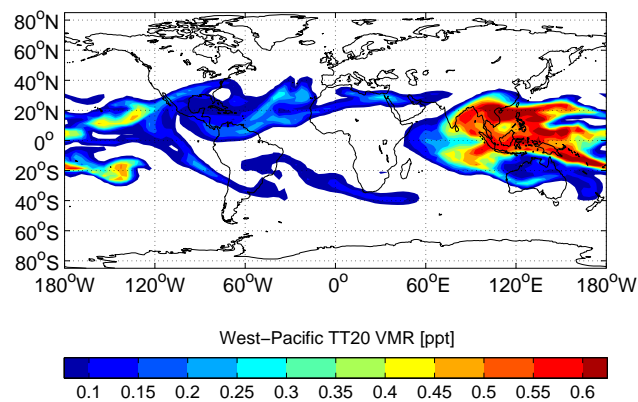


**Fig. 13.** Snapshot of the Western Pacific source gas tracer (TT20) distribution at 380 K on 4 December 2005.

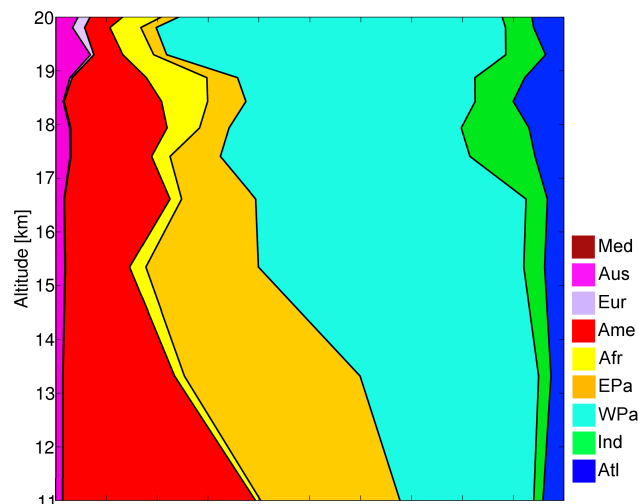


**Fig. 14.** Relative contribution of individual source regions to the total amount of TT20 (idealized bromoform tracer) in January/February 2004 above 80–90° W, 20° N–3° S (area of Pre-AVE campaign, see also Fig. 5).

#### 4 Discussion and conclusions

We have successfully implemented deep convective transport into an isentropic CTM. This allows us to study the transport of VSLs into the tropical UTLS in a physically motivated framework with large-scale transport constrained by diabatic heating rates and convective transport taking place in fast isolated updrafts. In this study we focussed on two idealized tracers whose chemical lifetime roughly corresponds to bromoform and methyl iodide but this approach can be easily extended to other VSLs as well.

An initial validation of the model with observations of the VSLs bromoform and methyl iodide, ozone and water vapor shows in general good agreement (Figs. 5, 6, 8, resp.). There

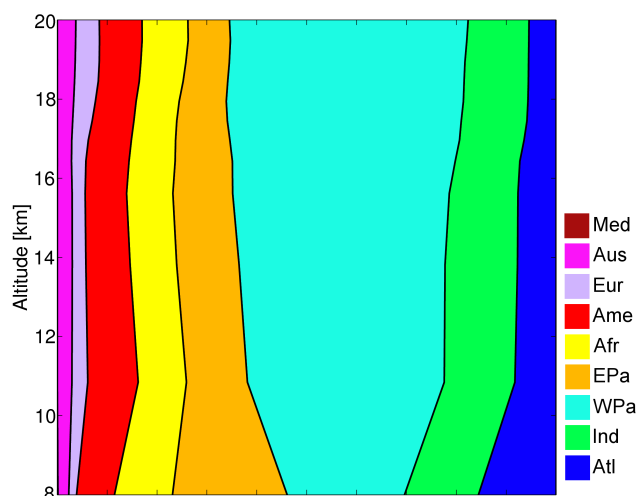


**Fig. 15.** Averaged relative contribution of individual source regions to the total amount of TT20 (idealized bromoform tracer) from 8–20 km in the tropics.

is some evidence from the ozone and water comparisons that could indicate too much convective transport into the 16 to 18 km altitude region. However, a comparison of the convective turnover time scales in the TTL from our model with estimates from Dessler (2002), based on  $O_3$  and CO observations, shows excellent agreement (Fig. 3), so it may also be that existing deviations from ozone and water vapor observations are a consequence of our simplified approach in the treatment of these species. Furthermore, a sensitivity calculation with convective detrainment set to zero above 380 K altitude shows that our main results are not dependent on the amount of convective transport to altitudes above the cold-point (Fig. 10).

Comparisons with recent model studies show also in general good agreement with our results taking into account the differences in the modeling approaches, source strengths, lifetimes and other parameters. Estimations of the amount of bromoform reaching the tropical stratosphere ( $CHBr_3$  abundance at 18 km altitude) are ranging from 0.1 ppt (Warwick et al., 2006) over 0.15 ppt (Hossaini et al., 2009) up to 0.5 ppt (Gettelman et al., 2009) with our results of 0.1 ppt residing at the lower bound.

Our main result is an estimation of the impact of dehydration on  $Br_y$  from VLSL entering the stratosphere. Given the commonly used assumption of a bromoform mixing ratio of 1 ppt at ground-level, we constrain the stratospheric bromine loading due to bromoform (TT20) to 1.6 to 3 ppt (Fig. 10). Note that complete solubility and instantaneous washout only removes about 50% of the  $Br_y$  transported into the stratosphere compared to the insoluble tracer. Considering the lower limit of bromine loading due to the soluble  $Br_y$  tracer of 1.6 ppt we estimate that about 1.2 to 1.3 ppt is

originated from source gas injection whereas the remaining 0.3 to 0.4 ppt are from product gas injection. Comparing the estimations for bromine loading due to VLSL with previous work is difficult because of some significant differences between the conducted studies. Warwick et al. (2006) give an estimation of 6 to 7 ppt of additional inorganic bromine due to VSL bromocarbons at about 18 km (for bromoform only about 3.4 to 4 ppt). Gettelman et al. (2009) give a range of 1.1 to 4.1 ppt (bromoform only: 0.3 to 2.1 ppt) for the same quantity. Our estimations of additional bromine loading due to bromoform (1.6 to 3 ppt) are in between.

Finally we applied the bromoform degradation approach to different emission scenarios. We have identified the regions with most effective transport, e.g. the Western Pacific with a relative contribution of 55% (Fig. 15) assuming a uniform source. Along with the evidence that horizontal transport plays an utterly important role in the TTL (Fig. 13) we can confirm that the Western Pacific and the Maritime Continent are the most important pathways into the whole TTL and finally the stratosphere especially for short-lived substances.

With our current study we have established a modeling tool to further investigate the transport and transformation of VLSL into the stratosphere. The comparison with VLSL measurements indicates that we can successfully reproduce the source gas input of VLSL into the tropical UTLS. A next step would be a more sophisticated treatment of  $Br_y$  uptake on ice with subsequent sedimentation and the inclusion of more realistic VLSL emission scenarios.

*Acknowledgements.* J. A. acknowledges financial support by the University of Bremen through project VLSL. Parts of this work were supported by the EU projects SCOUT-O3 and SHIVA. ERA-Interim data were provided through the ECMWF special project DECDIO. Measurements of halocarbons were supported by the NASA Upper Atmosphere Research Program. We thank R. Lueb for field support, and X. Zhu and L. Pope for analytical work.

Edited by: M. Dameris

## References

- Chipperfield, M. P.: New Version of the TOMCAT/SLIMCAT Off-Line Chemical Transport Model: Intercomparison of Stratospheric Tracer Experiments, *Q. J. Roy. Meteor. Soc.*, 132, 1179–1203, doi:10.1256/qj.05.51, 2006.
- Corti, T., Luo, B. P., Peter, T., Fu, Q., and Vömel, H.: Mean radiative energy balance and vertical mass fluxes in the equatorial upper troposphere and lower stratosphere, *Geophys. Res. Lett.*, 32, L06802, doi:10.1029/2004GL021889, 2005.
- Dessler, A. E.: The effect of deep, tropical convection on the tropical tropopause layer, *J. Geophys. Res.*, 107(D3), 4033, doi:10.1029/2001JD000511, 2002.
- Dessler, A. E. and Sherwood, S. C.: Effect of convection on the summertime extratropical lower stratosphere, *J. Geophys. Res.*, 109, D23301, doi:10.1029/2004JD005209, 2004.
- Folkens, I., Kelly, K. K., and Weinstock, E. M.: A simple explanation for the increase in relative humidity between 11 and 14 km in

- the tropics, *J. Geophys. Res.*, 4736, doi:10.1029/2002JD002185, 2002.
- Fueglistaler, S., Bonazzola, M., Haynes, P. H., and Peter, T.: Stratospheric water vapor predicted from the Lagrangian temperature history of air entering the stratosphere in the tropics, *J. Geophys. Res.*, 110, D08107, doi:10.1029/2004JD005516, 2005.
- Fueglistaler, S., Legras, B., Beljaars, A., Morcrette, J.-J., Simmons, A., Tompkins, A. M., and Uppala, S.: The diabatic heat budget of the upper troposphere and lower/mid stratosphere in ECMWF reanalyses, *Q. J. Roy. Meteor. Soc.*, 135(638), 21–37, 2009.
- Gottelman, A., Randel, W. J., Wu, F., and Massie, S. T.: Transport of water vapor in the tropical tropopause layer, *Geophys. Res. Lett.*, 29(1), 1009, doi:10.1029/2001GL013818, 2002a.
- Gottelman, A., Salby, M. L., and Sassi F.: The distribution and influence of convection in the tropical tropopause region, *J. Geophys. Res.*, 107(D10), 4080, doi:10.1029/2001JD00104, 2002b.
- Gottelman, A., Lauritzen, P. H., Park, M., and Kay, J. E.: Processes regulating short-lived species in the tropical tropopause layer, *J. Geophys. Res.*, 114, D13303, doi:10.1029/2009JD011785, 2009.
- Groß, J.-U. and Russell, J. M. III: Technical note: A stratospheric climatology for O<sub>3</sub>, H<sub>2</sub>O, CH<sub>4</sub>, NO<sub>x</sub>, HCl and HF derived from HALOE measurements, *Atmos. Chem. Phys.*, 5, 2797–2807, 2005, <http://www.atmos-chem-phys.net/5/2797/2005/>.
- Hanisco, T. F., Moyer, E. J., Weinstock, E. M., St. Clair, J. M., Sayres, D. S., Smith, J. B., Lockwood, R., Anderson, J. G., Dessler, A. E., Keutsch, F. N., Spackman, J. R., Read, W. G. and Bui, T. P.: Observations of deep convective influence on stratospheric water vapor and its isotopic composition, *Geophys. Res. Lett.*, 34, L04814, doi:10.1029/2006GL027899, 2007.
- Holton, J. R. and Gottelman, A.: Horizontal transport and the dehydration of the stratosphere, *Geophys. Res. Lett.*, 28, 2799–2802, 2001.
- Hossaini, R., Chipperfield, M. P., Monge-Sanz, B. M., Richards, N. A. D., Atlas, E. and Blake, D. R.: Bromoform and dibromomethane in the tropics: a 3-D model study of chemistry and transport, *Atmos. Chem. Phys. Discuss.*, 9, 16811–16851, 2009, <http://www.atmos-chem-phys-discuss.net/9/16811/2009/>.
- IFS Documentation – Cy31r1, [www.ecmwf.int/research/ifsdocs/CY31r1/PHYSICS/IFSPart4.pdf](http://www.ecmwf.int/research/ifsdocs/CY31r1/PHYSICS/IFSPart4.pdf), last access: 14 August 2009, 2007.
- Kerkweg, A., Jöckel, P., Warwick, N., Gebhardt, S., Brenninkmeijer, C. A. M., and Lelieveld, J.: Consistent simulation of bromine chemistry from the marine boundary layer to the stratosphere – Part 2: Bromocarbons, *Atmos. Chem. Phys.*, 8, 5919–5939, 2008, <http://www.atmos-chem-phys.net/8/5919/2008/>.
- Liu, C. and Zipser, E. J.: Global distribution of convection penetrating the tropical tropopause, *J. Geophys. Res.*, 110(D23), D23104, doi:10.1029/2005JD006063, 2005.
- Marti, J. and Mauersberger, K.: A survey and new measurements of ice vapor pressure at temperatures between 170 and 250 K, *Geophys. Res. Lett.*, 20, 363–366, 1993.
- McLinden, C. A., Olsen, S. C., Hannegan, B., Wild, O., Prather, M. J., and Sundet, J.: Stratospheric ozone in 3-D models: A simple chemistry and the cross-tropopause flux, *J. Geophys. Res.*, 105(D11), 14653–14665, 2000.
- Nielsen, J. E. and Douglass, A. R.: A simulation of bromoform's contribution to stratospheric bromine, *J. Geophys. Res.*, 106(D8), 8089–8100, 2001.
- Quack, B., and Wallace, D. W. R.: Air-sea flux of bromoform: Controls, rates, and implications, *Global Biogeochem. Cycles*, 17(1), 1023, doi:10.1029/2002GB001890, 2003.
- Rasch, P. J., Mahowald, N. M., and Eaton, B. E.: Representations of transport, convection, and the hydrologic cycle in chemical transport models: Implications for the modeling of short-lived and soluble species, *J. Geophys. Res.*, 102(D23), 28127–28138, 1997.
- Read, W. G., Schwartz, M. J., Lambert, A., Su, H., Livesey, N. J., Daffer, W. H., and Boone, C. D.: The roles of convection, extratropical mixing, and in-situ freeze-drying in the tropical tropopause layer, *Atmos. Chem. Phys.*, 8, 6051–6067, 2008, <http://www.atmos-chem-phys.net/8/6051/2008/>.
- Sinnhuber, B.-M., Weber, M., Amankwah, A., and Burrows, J. P.: Total ozone during the unusual Antarctic winter of 2002, *Geophys. Res. Lett.*, 30(11), 1580, doi:10.1029/2002GL016798, 2003.
- Sinnhuber, B.-M. and Folkins, I.: Estimating the contribution of bromoform to stratospheric bromine and its relation to dehydration in the tropical tropopause layer, *Atmos. Chem. Phys.*, 6, 4755–4761, 2006, <http://www.atmos-chem-phys.net/6/4755/2006/>.
- Sinnhuber, B.-M., Sheode, N., Sinnhuber, M., Chipperfield, M. P., and Feng, W.: The contribution of anthropogenic bromine emissions to past stratospheric ozone trends: a modelling study, *Atmos. Chem. Phys.*, 9, 2863–2871, 2009, <http://www.atmos-chem-phys.net/9/2863/2009/>.
- Thompson, A. M., Witte, J. C., McPeters, R. D., Oltmans, S. J., Schmidlin, F. J., Logan, J. A., Fujiwara, M., Kirchhoff, V. W. J. H., Posny, F., Coetzee, G. J. R., Hoegger, B., Kawakami, S., Ogawa, T., Johnson, B. J., Vömel, H. and Labow, G.: Southern Hemisphere Additional Ozonesondes (SHADOZ) 1998–2000 tropical ozone climatology I. Comparison with Total Ozone Mapping Spectrometer (TOMS) and ground-based measurements, *J. Geophys. Res.*, 108(D2), 8238, doi:10.1029/2001JD000967, 2003.
- Warwick, N. J., Pyle, J. A., Carver, G. D., Yang, X., Savage, N. H., O'Connor, F. M., and Cox, R. A.: Global modeling of biogenic bromocarbons, *J. Geophys. Res.*, 111, D24305, doi:10.1029/2006JD007264, 2006.
- WMO (World Meteorological Organization): Scientific Assessment of Ozone Depletion: 2006, Global Ozone Research and Monitoring Project-Report No. 50, 572 pp., Geneva, Switzerland, 2007.